Article

The fabrication and characterization of stable core-shell superparamagnetic nanocomposites for potential application in drug delivery

Eizadi Sharifabad, M, Mercer, Tim and Sen, Tapas

Available at http://clok.uclan.ac.uk/12093/

It is advisable to refer to the publisher's version if you intend to cite from the work.
http://dx.doi.org/10.1063/1.4917264

For more information about UCLan's research in this area go to
http://www.uclan.ac.uk/researchgroups/ and search for <name of research Group>.

For information about Research generally at UCLan please go to
http://www.uclan.ac.uk/research/

CLoK
Central Lancashire online Knowledge
www.clok.uclan.ac.uk

The fabrication and characterization of stable core-shell superparamagnetic nanocomposites for potential application in drug delivery

M. Eizadi Sharifabad,[1] T. Mercer,[1,2,a)] and T. Sen[1]

[1]Centre for Materials Science, University of Central Lancashire, Preston PR1 2HE, United Kingdom
[2]Jeremiah Horrocks Institute for Mathematics, Physics and Astronomy, University of Central Lancashire, Preston PR1 2HE, United Kingdom

Two systems of core-shell superparamagnetic nanoparticles in the size range of 45–80 nm have been fabricated by the coating of bare magnetite particles with either mesoporous silica or liposomes and the loading/release of the anti-cancer drug Mitomycin C (MMC) from their surfaces has been investigated. The magnetic cores of size $\sim$10 nm were produced by a co-precipitation method in aqueous solution, with the silica coating containing an unstructured network of pores of size around 6 nm carried out using a surfactant-templating approach and the liposome coating achieved by an evaporation-immersion technique of the particles in a lipid solution. Stability measurements using a scanning column magnetometry technique indicated that the lipid-coating of the particles halts the sedimentation otherwise apparent in <1 h for the bare magnetite to produce an ultra-stable system and thereby overcome one of the main barriers to potential *in-vivo* applications. Whilst an increase in stability was also observed in the silica-coated system, it was still unstable over a few hours and will require further investigation. Magnetization curves of the coated systems were indicative of superparamagnetic behavior whilst the i*n vitro* loading and release of MMC resulted in two distinctly different outcomes for the two systems: (i) the silica-coated particles saturated in <4 h to a loading of around 7 μg/mg of material, releasing about 6% at a near constant rate over 48 h whilst (ii) the lipid-coated particles saturated to around only 4 μg/mg over the same time period but with a subsequent rapid release rate over the first 3 h to 27% then rising near-linearly to a value of about 45% at the 48 h mark. This gives scope for systems' to be tuned to the appropriate rate and load delivery as required by clinical need with further investigations underway. © 2015 AIP Publishing LLC. [http://dx.doi.org/10.1063/1.4917264]

I. INTRODUCTION

The need for bio-compatible superparamagnetic particles in the diameter, d, range $(10 \leq d \leq 100)$ nm continues to be an important field of study for biomedical applications such as hyperthermia, contrasting agents and bio-molecule separation.[1–3] For potential applications in drug delivery, the surface of a nanoparticle needs to satisfy a number of essential functions, namely, (i) to have an acceptably low toxicity in an aqueous suspension, (ii) to enable the drug of choice to be bound to the surface, and (iii) to provide colloidal stability. This last point is crucial because it ensures that the coating is covering individual particles rather than agglomerates and thereby maintains a high surface area and consistent particle size of $<$ 100 nm. The upper size limit is a key parameter, as it allows the particle to be small enough to diffuse through the cell membrane[4] and, in conjunction with the lower limit of $d > 10$ nm, prolongs circulation time in the blood by the avoidance of the body's reticuloendothelial system.[5]

In order to obtain particles that have both the necessary superparamagnetic and surface properties, composites of a magnetic core coated with either an organic or inorganic layer (core-shell) are ideal candidates. Of these, iron oxide cores of either magnetite (Fe_3O_4) or maghemite (γ-Fe_2O_3) are commonly used as they are already in an oxidized state, are non-toxic and on the nanoscale their bulk ferrimagnetic properties reduce to that of single domain, uniaxial superparamagnetic nanoparticles.[6] In this state, the particles effectively have no magnetic moment in zero applied field at room temperature, but respond to an external field to the extent that they can be targeted at a site using a high gradient static field.[4]

Silica coatings with a mesoporous network of pores and channels offer favorable properties for drug delivery due to their non-toxic nature combined with a high surface area and controllable functionality.[7] Mesopores of 3–10 nm are potentially the best size as most drugs or biomolecules fit within that size range and thereby overcome any diffusional restriction. Likewise, liposome coatings are also good candidates with well-known drug delivery properties and the ability to increase stability in suspension by the modification of surface charge.[8,9] However, as most investigations involve composites of size $>$ 100 nm there is a real need for fabrication and study in the sub 100 nm range if diffusion through the target cell membrane is to be achieved.

In the work reported here, the fabrication and characterization of core-shell superparamagnetic nanocomposites in the range of 45–80 nm is detailed for both lipid-coated and mesoporous silica-coated iron oxide nanoparticles. The effects on stability due to coating are investigated along with and the *in vitro* loading and releasing of the anti-cancer drug Mitomycin C.

a)Electronic mail: tmercer1@uclan.ac.uk.

II. EXPERIMENTAL DETAILS

All chemicals were purchased from Sigma-Aldrich and used without further purification.

A. Synthesis of core-shell superparamagnetic iron oxide nanoparticles

Superparamagnetic Iron Oxide Nanoparticles (SPIONs) were synthesized by co-precipitation of an aqueous solution of ferrous and ferric chloride in the presence of ammonium hydroxide, with full details reported elsewhere.[9] Briefly, 8.46 g of $FeCl_2 \cdot 4H_2O$ and 22.95 g of $FeCl_3 \cdot 6H_2O$ was dissolved in 500 ml of degassed and deionized water under a nitrogen environment. The mixture was stirred in an oil bath at 80 °C. A volume of 50 ml of aqueous ammonium hydroxide (25% w/v NH_4OH) was added drop-wise to the mixture over 30 min. The reaction was allowed to proceed for a further 1 h. The black reaction products were collected and washed several times in deionized water using magnetic separation. The final product had a pH ~ 7.

Liposome coatings were prepared by dissolving 66 mg of SPC phospholipid and 34 mg of cholesterol in 3.96 ml of chloroform in a 500 ml round bottom flask. The flask containing the phospholipid solution was attached to a rotary evaporator and immersed in a 41 °C water bath for 1 h. Upon evaporation of chloroform, a thin film of lipid formed on the inner wall of the flask. The film was hydrated with 10 ml of deionized water and shaken manually for 10 min followed by annealing for 2 h at room temperature. After that, 1 ml of magnetite (6.03 mg/ml) was diluted with 0.7 ml water and added to the liposome solution. The mixture was then placed in an ice bath under strong ultrasonic vibration (titanium horn) for 8 min.

The mesoporous silica shell coating was fabricated on the surface of the magnetic nanoparticles through a surfactant-templating approach. In this method, 225 mg of core magnetite was suspended in 300 ml of water and 45 ml of a solution containing sodium hydroxide (0.22 M) and cetyltrimethylammonium bromide (CTAB) (0.049 M) was added to the nanoparticles while stirring, with stirring continued for a further 30 min. A subsequent 3.78 g of tetraethyl orthosilicate (TEOS) was added drop-wise to the mixture and the reaction left stirring continually for 8 h at room temperature before adding 2 M of HCl drop-wise to make a final solution with a pH of 7. The mixture was stirred for an extra 30 min before being rinsed twice with 500 ml of a 1:1 mixture of deionized water and ethanol in order to remove the surfactant from the mesopores as reported earlier[10] and followed by subsequent washing with deionized water.

B. Characterization, stability, and drug loading/release measurements

SPION composition was determined by X-ray diffraction (XRD) using Cu K_α radiation. Nitrogen adsorption and desorption using a Micromeritics ASAP 2010 was used to determine the specific surface area and pore size of the silica coatings by Brunauer-Emmett-Teller (BET) and Barrett-Joyner-Halenda (BJH) techniques, respectively. The structure of the coating was determined by small angle X-ray scattering (SAXS) using Cu K_α radiation.

Magnetisation measurements were carried out using an in-house 6 kOe vibrating sample magnetometer (VSM) with stability observations of a column of the aqueous particle suspensions determined using a scanning column magnetometry (SCM) technique. Vertically held glass tubes of internal diameter 11 mm were filled to produce a column of height ~ 100 mm, which was then placed in the SCM. Further details of the SCM method are given elsewhere,[11] but briefly this involves driving the column of magnetic particles down through the otherwise empty core of a coil that forms part of a tuned resonance circuit. The introduction of magnetic material into the core causes a change to the coil inductance and a corresponding shift in the resonance frequency, ΔF, from its sample-free value of 1 MHz. As this shift is directly proportional to the magnetic particle concentration, a plot of ΔF as a function of column height gives the complete concentration profile of the colloid. It is by recording a series of these profiles over time that any sedimentation of the suspension may be investigated.

Transmission electron microscopy (TEM) was carried out on a JEOL JEM2000EX system at an operating voltage of 200 kV with the samples prepared from suspension by being pipette-dropped onto a carbon-coated copper grid and allowed to dry at room temperature prior to imaging. Particle size analysis for the lipid-coated systems was carried out by dynamic light scattering using a Malvern Instruments Zetasizer Nano.

Loading of the MMC drug on the liposome-coated particles and the silica-coated particles was carried out using an incubation method described in detail previously,[9] except at a temperature of 10 °C instead of 25 °C. In both cases, the amount of MMC loading was determined by measuring the UV absorption at 365 nm ($\lambda_{365\,nm}$) at different time intervals until saturation was reached and with the concentration values found from comparison with a pre-established standard curve of known MMC concentrations in water. MMC-loaded nanoparticles from each of the two types of coatings were separated from the reaction solution by magnetic separation and washed with deionized water prior to use in the release study.

Release of the loaded drug was carried out in a Phosphate Buffered Saline (PBS) solution ($7.1 \geq pH \geq 7.2$) of 1 ml added to 4 mg of washed nanoparticles under stirring by end-over-end rotation for up to 48 h at 37 °C. Concentration values were again determined from UV $\lambda_{365\,nm}$ absorption values, but this time from a known standard curve of MMC in PBS buffer.

III. RESULTS AND DISCUSSION

TEM micrographs show bare iron oxide cores of size 8–12 nm as can be seen in Fig. 1(a). In Fig. 1(b), micrographs of the silica-coated particles show the composite diameter to be around 45 nm, with multiple cores apparent in a consistent size and shape that are fully coated. Results from dynamic light scattering showed a mono-modal distribution centered on 80 nm as the composite size of the lipid-coated particles. As lipid coatings need to be hydrated in order to estimate their *in-situ* composite size, the dry-sample TEM method used for the other systems was not applicable here.

XRD measurements on the bare (uncoated) particles are shown in part (c) of Fig. 1. These show clear peaks indicating a crystalline structure of either Magnetite (Fe_3O_4) or
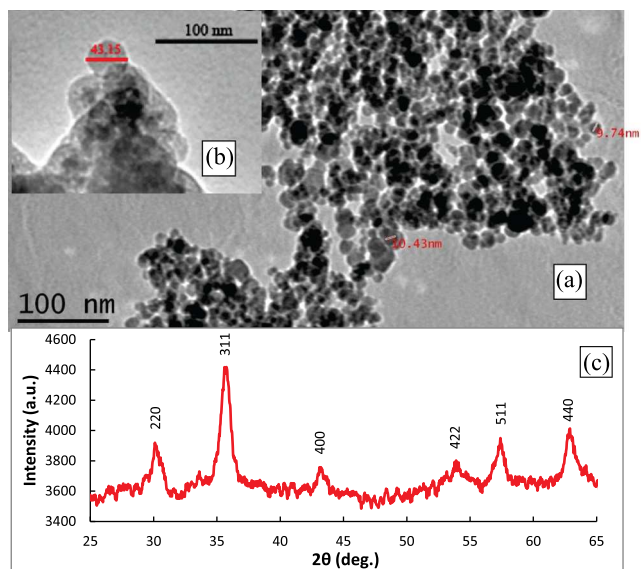
FIG. 1. TEM micrographs of (a) the uncoated iron oxide nanoparticles and (b) the silica-coated composite. The XRD pattern of the uncoated particles and its indices is shown in (c).

FIG. 3. SCM concentration profiles of the unstable bare magnetite suspension in the main plot and the stable lipid-coated suspension of the inset.

Maghemite (γ-Fe$_2$O$_3$) or a mixture of the two,[12] which in either of these cases provides the superparamagnetic properties required of these iron oxide systems.

Characterization of the silica coatings using SAXS is given in Fig. 2(a). In the low angle range shown, it is evident that there is a small feature between the 2θ values of 1.0–1.5 degrees. Analysis using the magnitude of the Q scattering vector can be seen in the inset of the same figure, showing this feature to be equivalent to a size of nearly 6 nm. However, the lack of a sharp and well defined peak is indicative of a lack of order in this feature, as would be expected in a disordered mesoporous structure, and is also consistent with the lack of distinctive rings observed in the scattering pattern (not shown). Further measurements on the structure and characterization of the silica shell are shown in the nitrogen adsorption and desorption curves as a function of relative pressure given in Fig. 2(b). The hysteresis observed is indicative of a porous structure, which was quantified using BJH analysis to yield a pore size of 7 nm that compares well with the size of approximately 6 nm determined using SAXS. Standard BET analysis showed the surface area of these silica coatings to be 134 m^2 g^{-1}.

Magnetic particle concentration profiles of resonance frequency shift as a function of suspension column height are shown in Fig. 3. By recording cumulative profiles of the same colloid sample over time, any sedimentation will be apparent due to the build-up of material at the bottom of the column. This is indeed the case for the bare particle profiles of the main plot, with Stokes-like sedimentation evident in less than 1 h as indicated by the reduction in concentration throughout the top layers and with no fall of any "sludge line" as would be observed in hindered settling systems.[13] The stability measurements for the lipid-coated system are shown in the inset of Fig. 3 indicating a stable state has been achieved with no sedimentation evident at >30 h. Whilst an increase in stability to a few hours was observed in the silica-coated suspension (not shown), this will need to be increased if potential *in vivo* applications are to be realized. However, the bio-molecule compatibility of the mesoporous surface means that this warrants further investigation and is the subject of current investigations.

Magnetization curves are shown in Fig. 4, comparing the uncoated particles of the main plot with the silica-coated system of the inset. Some hysteresis, albeit small, is clearly evident in the bare particle assembly, which would not normally be expected in iron oxide particles below about 15 nm in size as they are expected to be superparamagnetic.[5] However, if assemblies of nanoparticles are agglomerated/clustered close enough together then the increased strength of the magnetic dipolar interactions can cause a ferromagnetic-like state to emerge.[14] Such bigger assemblies would be consistent with
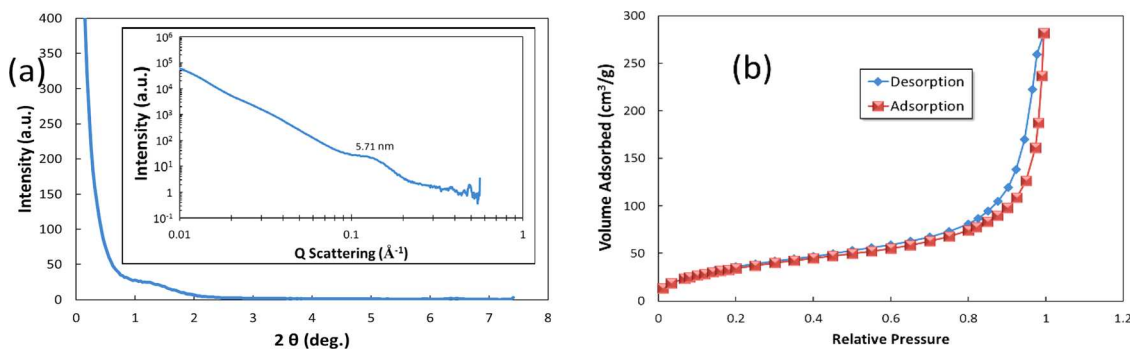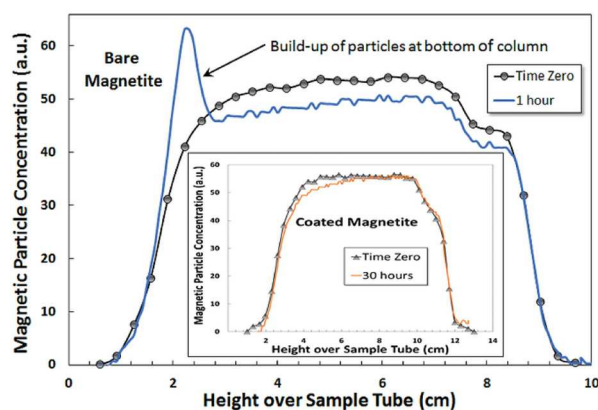

FIG. 2. The SAXS scattering intensity of (a) shows a small broad feature between 1.0 and 1.5° with the Q scattering analysis of the inset resulting in a mesoporous pore size of around 6 nm for the silica-coated particles. The nitrogen adsorption/desorption curves of (b) show hysteresis and thereby indicate the porous structure of the silica shell.
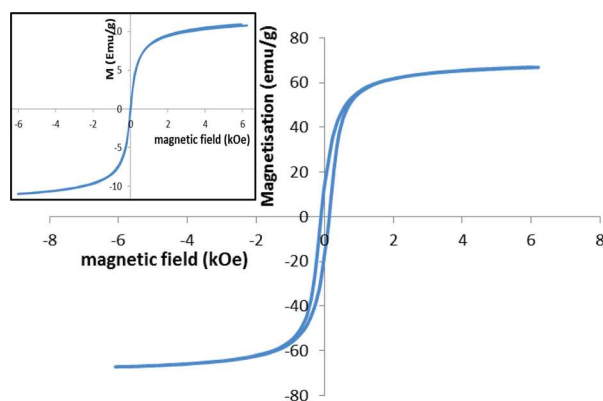
FIG. 4. Magnetization curves showing distinct, but small hysteresis for the bare magnetite of the main plot and a closed loop for the silica-coated system of the inset that is indicative of superparamagnetic behavior.

the lack of stability seen in the bare system of the main SCM plot of Fig. 3. Likewise, the similar closed loops of the silica-coated system (inset of Fig. 4) and the lipid-coated particles (not shown) is indicative of a superparamagnetic state and the increase in stability observed in both coated systems.

The results of the *in vitro* loading and release of the anti-cancer drug MMC are shown in Figs. 5(a) and 5(b), respectively, with any error bars that are significant on this scale estimated from the standard deviation of a minimum of three experiments in each case. From this, it can be seen that the silica-coated particles reached a rapid saturation loading of around 7 μg/mg of material in under 4 h, whereas after a similar initial rise, the lipid-coated particles took over 20 h to reach their loading limit of about 4 μg/mg. The loading effect for the silica-coated particles was optimized by reducing the

incubation temperature from 25 °C to 10 °C with the lipid-coated system also loaded at 10 °C for comparison. In general, the increase in loading by a reduction of the incubation temperature is consistent with the decrease in thermal energy and subsequent decrease in Brownian motion that allows the drug to be "captured" more easily at the surface. For the release study of Fig. 5(b), the silica-coated system is at, or near, a constant release rate after more than 25 h of around 6% and is predominantly flat over the whole time period. For the lipid-coated system, an initially rapid rise to about 27% after the first 3 h continues to rise at a slower, but near linear rate to reach around 45% at the 48 h point. Understanding the reasons for these differences is highly complicated when comparing systems of two different surfaces and requires an in-depth and systematic investigation that is currently underway. Nevertheless, this does indicate that there is a good deal of scope to tune the loading, rate and drug delivery levels to those required by clinical need.

IV. CONCLUSIONS

Two systems of lipid-coated and mesoporous silica-coated superparamagnetic core-shell nanocomposites have been fabricated in the size range $(45 \leq d \leq 80)$ nm that is within the limits $(10 \leq d \leq 100)$ nm required for potential drug delivery applications. The lipid-coated system was ultra-stable and capable of reaching *in vitro* MMC drug release levels at 45% of the loaded material. The silica-coated system did show an increase in stability compared to that of the uncoated nanoparticles used as the core, but will require modification to its surface properties before potential *in vivo* applications can be realized. However, its disordered mesoporous structure of pore size around 6 nm is highly compatible with drug and bio-molecules and warrants further study alongside the lower MMC drug release of approximately 6% of the loaded material. This gives scope for systems being tuned to the release rate and drug delivery level as defined by clinical need and is the subject of future work.
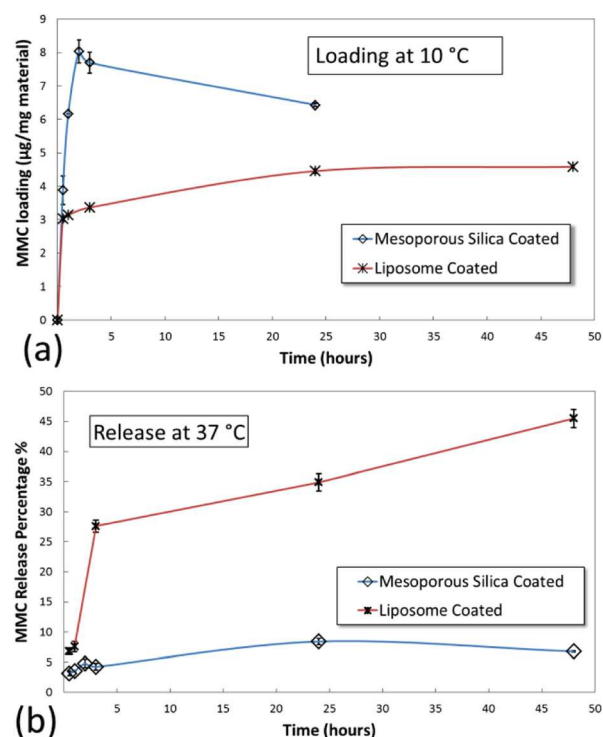
ACKNOWLEDGMENTS

(a)

(b)

FIG. 5. The *in vitro* loading (a) and release (b) of the drug MMC over time. The differences between the two systems give scope for these parameters to be changed as required by clinical need.

[1] R. M. Patil, P. B. Shete, N. D. Thorat *et al.*, J. Magn. Magn. Mater. **355**, 22 (2014).
[2] G. Gitsioudis, M. Stuber, I. Arend *et al.*, J. Magn. Reson. Imaging **38**, 836 (2013).
[3] F. Lan, Y. Wu, H. Hu *et al.*, RSC Adv. **3**, 1557 (2013).
[4] M. Mahmoudi, S. Sant, B. Wang *et al.*, Adv. Drug Deliver. Rev. **63**, 24 (2011).
[5] A. K. Gupta and M. Gupta, Biomaterials **26**, 3995 (2005).
[6] R. K. Zheng, H. Gu, B. Xu, and X. X. Zhang, J. Phys.: Condens. Matter **18**, 5905 (2006).
[7] M. Eizadi Sharifabad, B. Hodgson, M. Jellite *et al.*, Chem. Commun. **50**, 11185 (2014).
[8] P. Pradhan, J. Giri, R. Banerjee *et al.*, J. Magn. Magn. Mater. **311**, 208 (2007).
[9] T. Sen, S. J. Sheppard, T. Mercer *et al.*, RSC Adv. **2**, 5221 (2012).
[10] T. Sen, A. Sebastianelli, and I. J. Bruce, J. Am. Chem. Soc. **128**, 7130 (2006).
[11] T. Mercer and P. R. Bissell, IEEE Trans. Magn. **49**, 3516 (2013).
[12] W. Kim, C.-Y. Suh, S.-W. Cho *et al.*, Talanta **94**, 348 (2012).
[13] T. Mercer and P. R. Bissell, EPJ Web Conf. **40**, 01003 (2013).
[14] O. Petracic, Superlattices Microstruct. **47**, 569 (2010).